Surfaces and Interfaces:

Characterization of the Wettability of Solid Surfaces

Surface Wetting

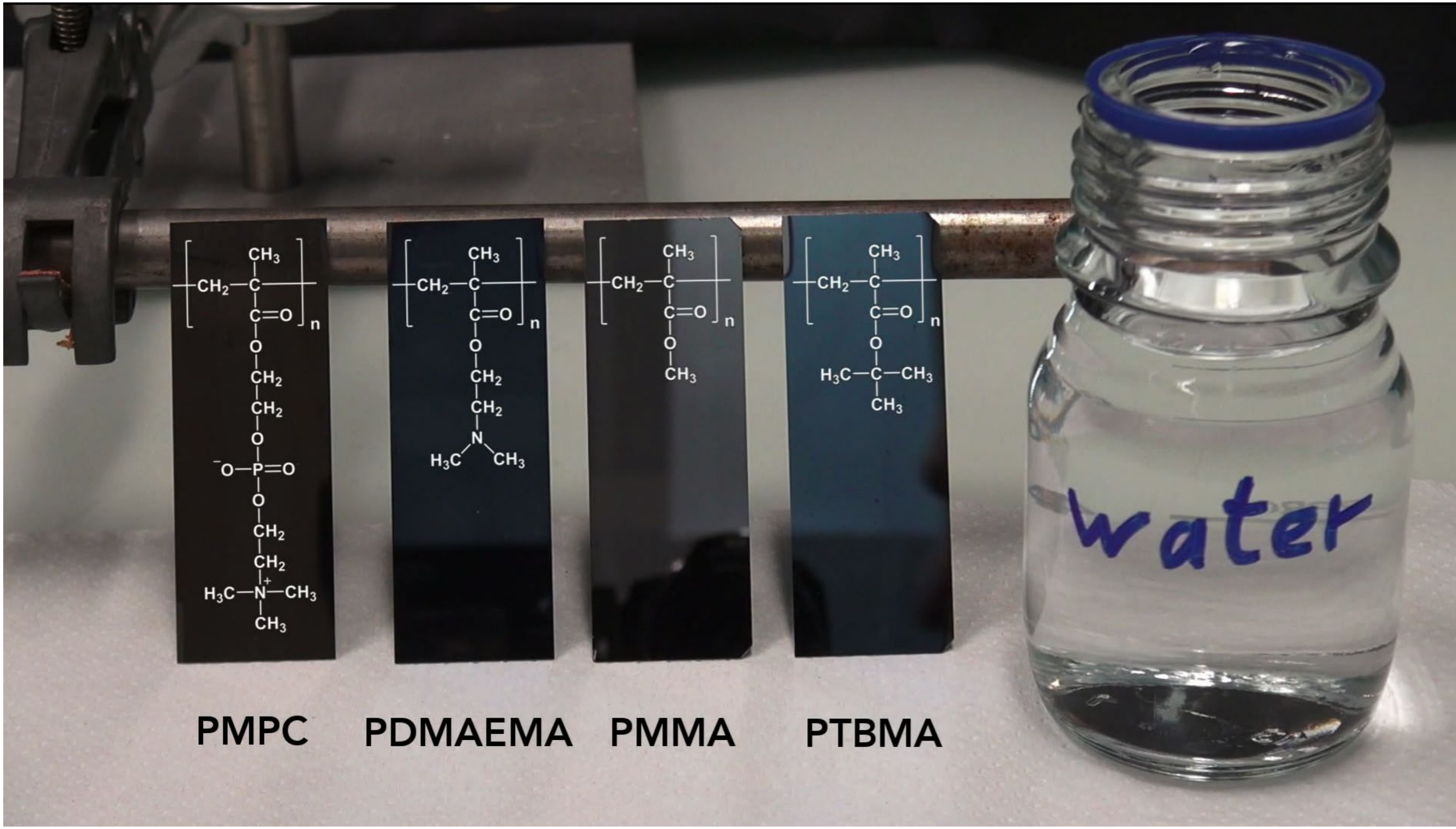

Film – Surface Wetting

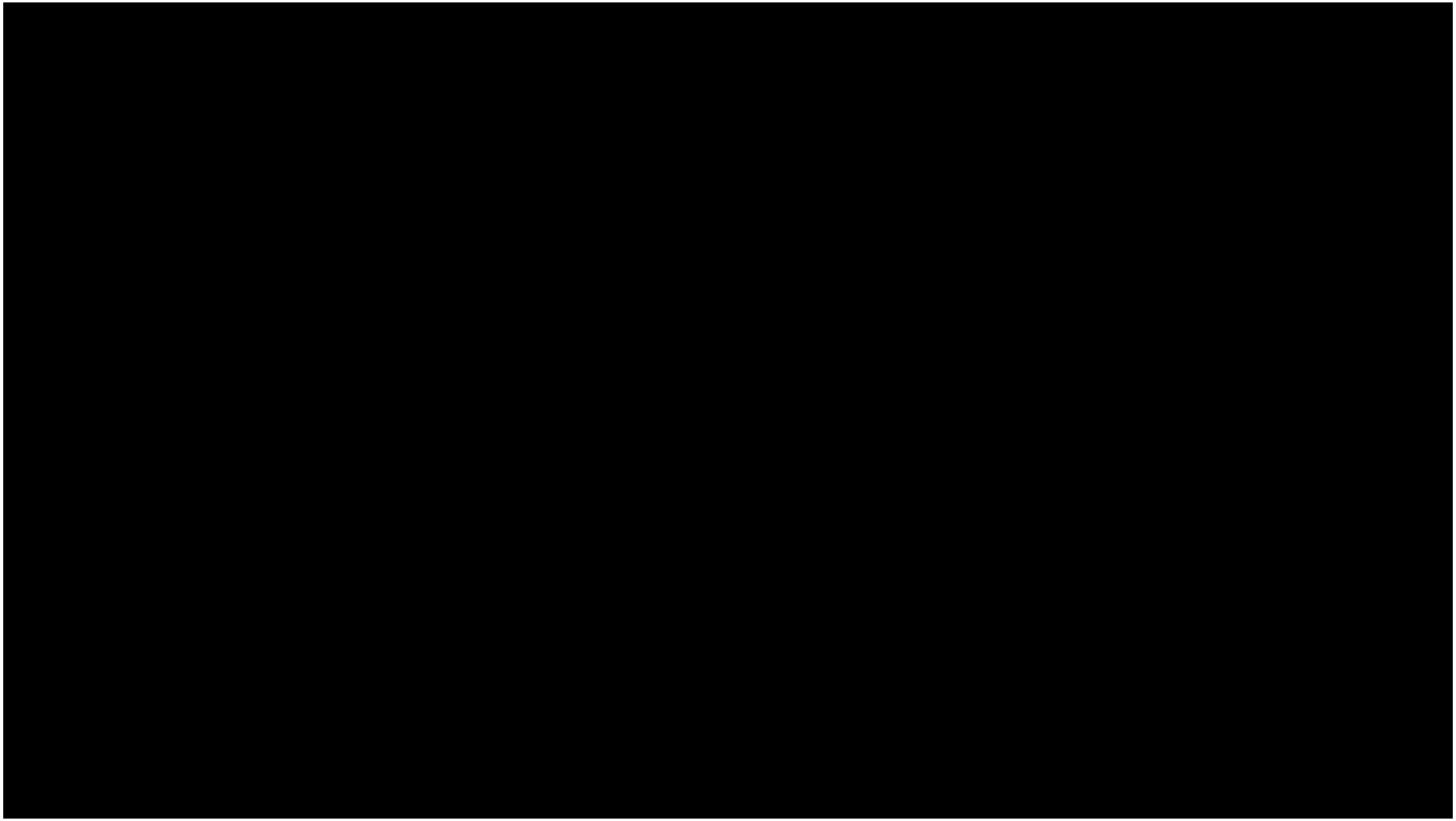

Water-proof, breathable textiles (Gore-Tex®)

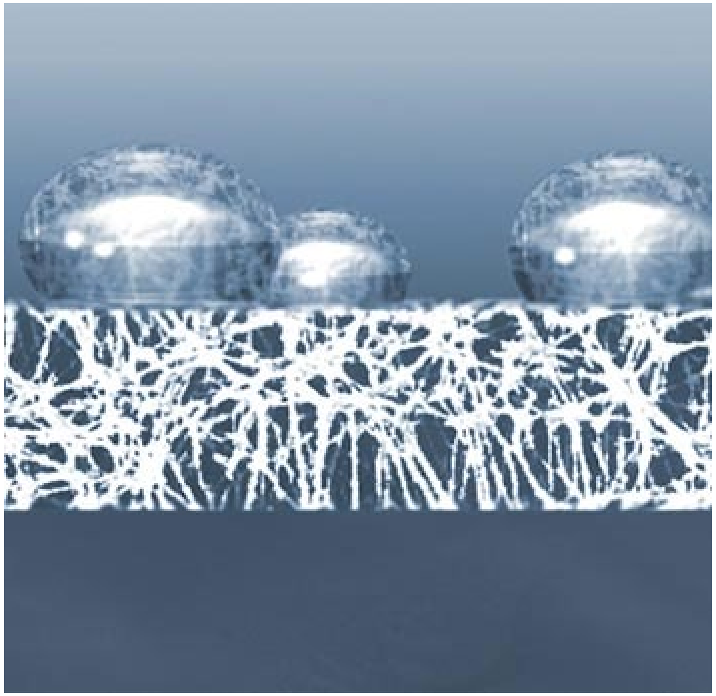

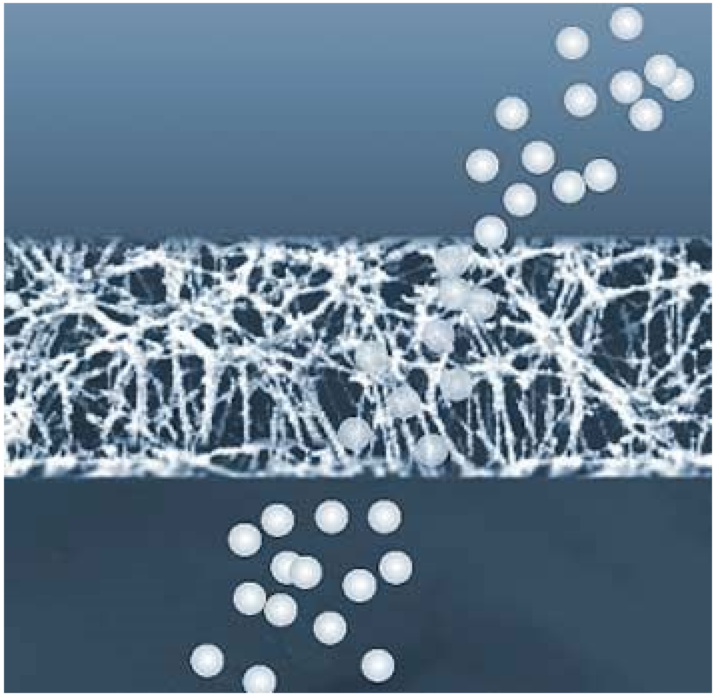

„GORE-TEX® products are based on GORE-TEX® ePTFE membrane technology. The membrane provides a thin, uniform barrier that can provide properties like waterproofness or chemical resistance. A single square inch of the GORE-TEX® membrane contains 9 billion microscopic pores — each 20,000 times smaller than a raindrop but 700 times larger than a molecule of water vapor — so while water can't pass through the fabric, perspiration can. Integrated into the ePTFE structure is an oleophobic, or oil-hating, substance that allows moisture vapor to pass through but is a physical barrier that prevents the penetration of contaminating substances such as oils, cosmetics, insect repellents, and food substances“

www.gore-tex.com

Outline

I: Introduction
II: Wetting/Dewetting Contact Angle
III: Characterization of Surfaces

Contact Angle

Measuring static and dynamic contact angle

Contact angle hysteresis

Young equation – Droplet size

Critical surface tension – Zisman plot

Surface roughness

Models of Wenzel and Cassie

J. Israelachvili, Intermolecular & Surface Forces, 2nd Edition, **1992**
S. Wu, Polymer Interface and Adhesion, Marcel Dekker, Inc. **1982**.

Contact Angle

Contact Angle – A three face boundary

- liquid-vapor (LV)
- solid-liquid (SL)
- solid-vapor(SV)

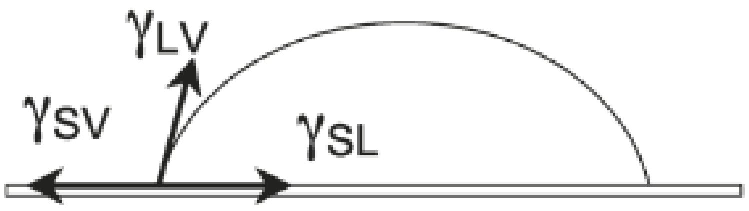

Variables/Challenges:

- drop size & drop height
- surface morphology
- evaporation time vs. measurement
- temperature and humidity
- surface impurities

L. Gao, T. J. McCarthy, *Langmuir* **2009**, 25, 14105.

Contact Angle

liquid = water

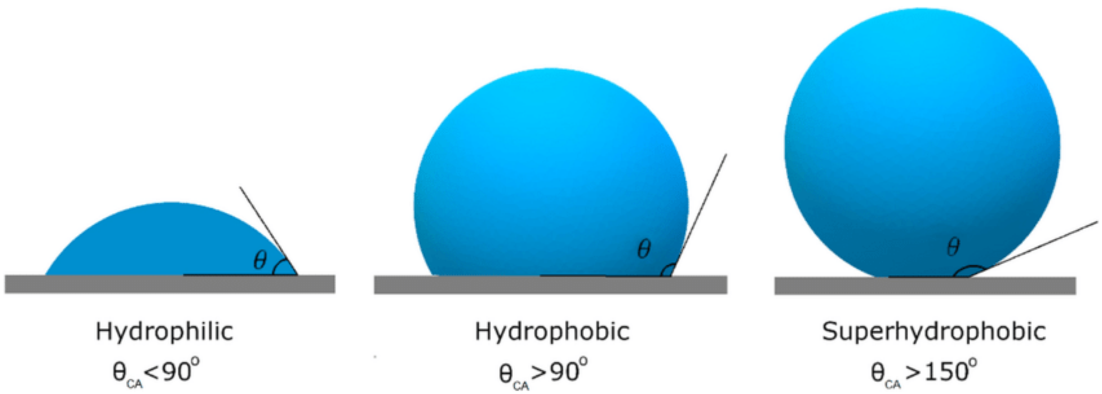

TABLE 3 Concerns in Contact Angle Measurement

The measurement is operator dependent.
Surface roughness influences the results.
Surface heterogeneity influences the results.
The liquids used are easily contaminated (typically reducing their ν_{lv}).
The liquids used can reorient the surface structure.
The liquids used can absorb into the surface, leading to swelling.
The liquids used can dissolve the surface.
Few sample geometries can be used.
Information on surface structure must be inferred from the data obtained.

Static and Dynamic Contact Angle

static contact angle

- Sessile drop on a substrate

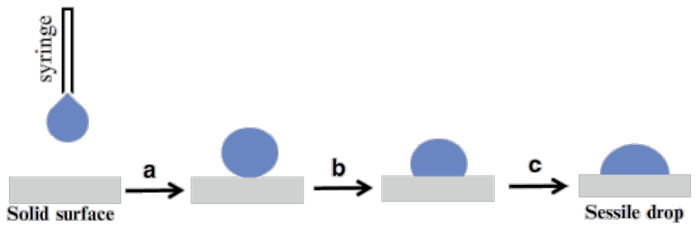

- captive bubble

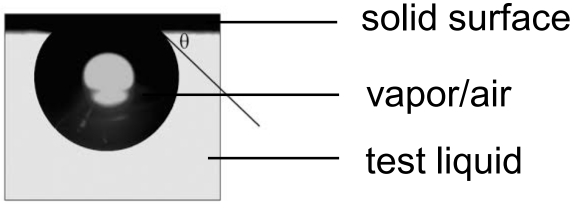

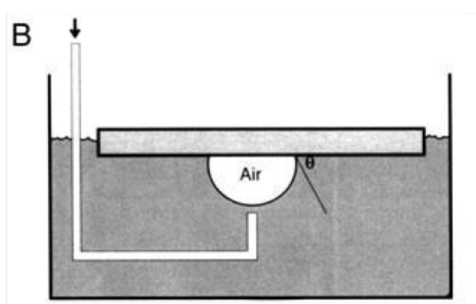

D. Y. Kwok, A. W. Neumann, *Adv. Colloid Interface Sci.* **1999**, 81, 167.

dynamic contact angle

- needle method

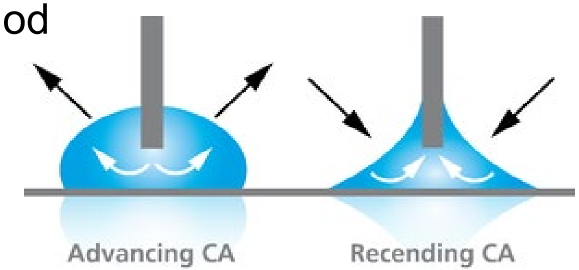

- tilting method

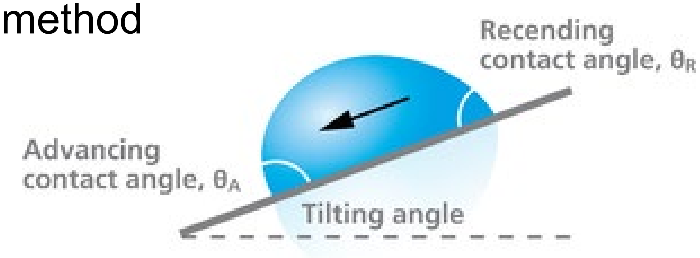

- Wilhelmy plate method

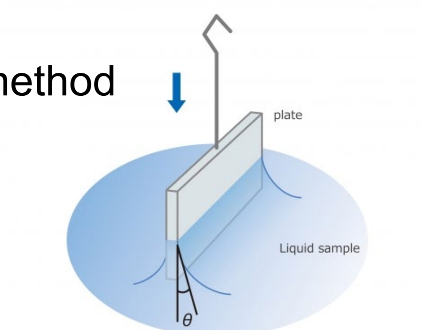

$$\gamma = \frac{F}{L\cos\theta}$$

Where:
γ : Surface tension
F : Measuring force (force acting on the plate)
L : Perimeter of plate
θ : Contact angle of plate and the liquid

Contact Angle Hysteresis

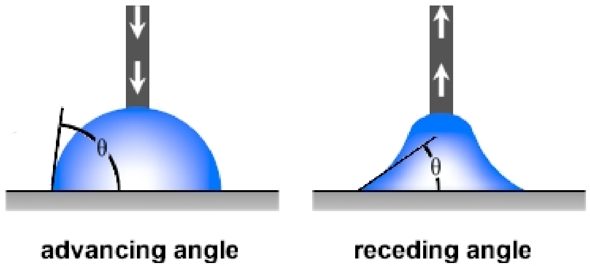

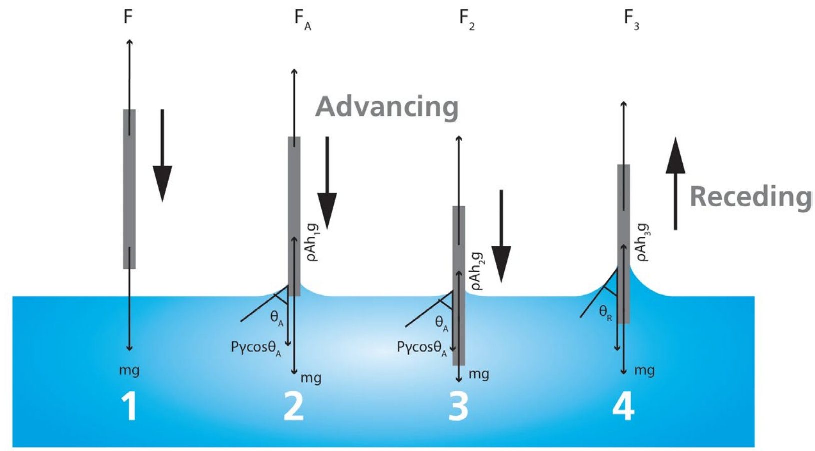

In dynamic liquid systems, a liquid front advancing across a new surface may exhibit a large contact angle (the advancing contact angle θ_A), while the same liquid receding from an already wetted surface will have a much smaller contact angle (the receding contact angle θ_R). The difference between θ_A and θ_R is termed the contact angle hysteresis.

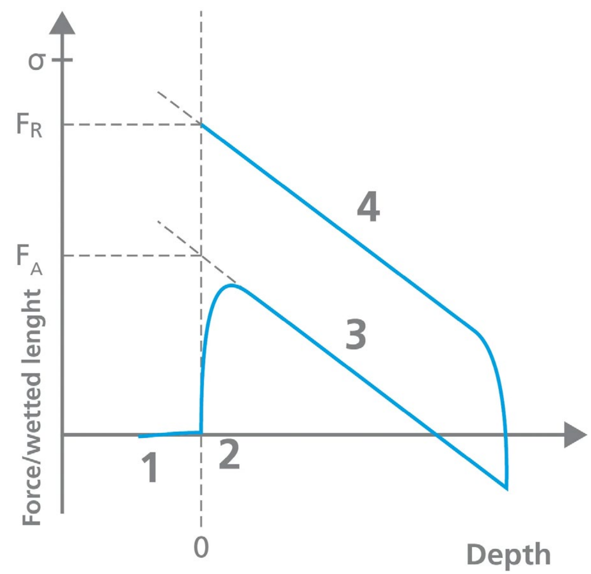

P is the perimeter of the plate,
γ is the surface tension of the liquid,
θ is the contact angle between the plate and the measured liquid,
ρ is the density of the liquid,
A is the surface area of the plate,
h the immersion depth, and
g the gravitational constant.

$$F(h) = P\gamma\cos\theta - \rho A h g$$

The first term on the right-hand side of the equation is caused by wetting force and the second by buoyancy.

Spreading Coefficient

Spreading refers to movement of a phase front whereby the interfacial area is increased.

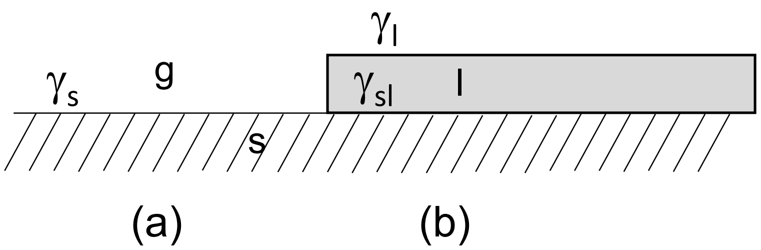

the surface free energy of (a) γ_s is per unit area and of (b) $\gamma_{sl} + \gamma_l$ where two interfaces are included. It is assumed that the spread liquid film is sufficiently thick such that the two interfaces are independent from each other (γ_l is of bulk liquid)

$$S = \lambda_{ls} = \gamma_s - \gamma_{sl} - \gamma_l$$

$S \geq 0$: liquid spreads completely – complete wetting

$S < 0$: no or partial wetting

Contact Angle Equilibrium: Young Equation

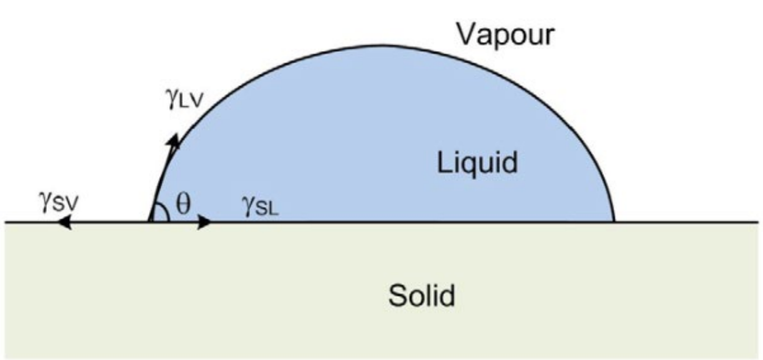

Stable equilibrium will be obtained if the solid surface is ideally smooth, homogenous, planar, and undeformable; the angle formed is the equilibrium contact angle.

$$\gamma_{lv}\, cos\theta = \gamma_{sv} - \gamma_{sl}$$

$$\cos\theta = \frac{\gamma_{sv} - \gamma_{sl}}{\gamma_{lv}}$$

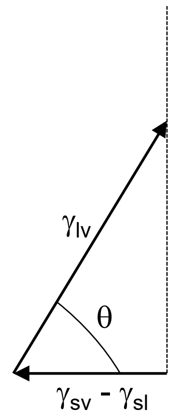

θ= 0° complete wetting

θ= 180° complete dewetting

With spreading coefficient: S = $\gamma_{lv}\,(cos\theta\ - 1)$

Forces in Droplets

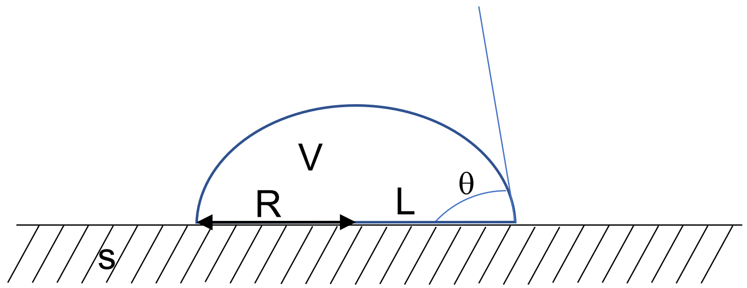

Droplet of radius R with a volume V.
Contact line L is a circle with radius R.

Forces at equilibrium of partial wetting:

horizontal: Young equation $\gamma_{lv}\, cos\theta = \gamma_{sv} - \gamma_{sl}$

and vertical : capillary forces on line L, Laplace pressure and gravity

$\gamma\ \sin\theta$ $\quad p_L \approx \dfrac{\gamma}{R}$ $\quad \rho g h$

From Droplets to Film

force equilibrium: $\gamma_s = \gamma_{sl} + \gamma_l - \frac{1}{2}\rho g h^2$

capillary length (or capillary constant) k^{-1}:

$$k^{-1} = (\frac{\gamma_l}{\rho g})^{1/2}$$

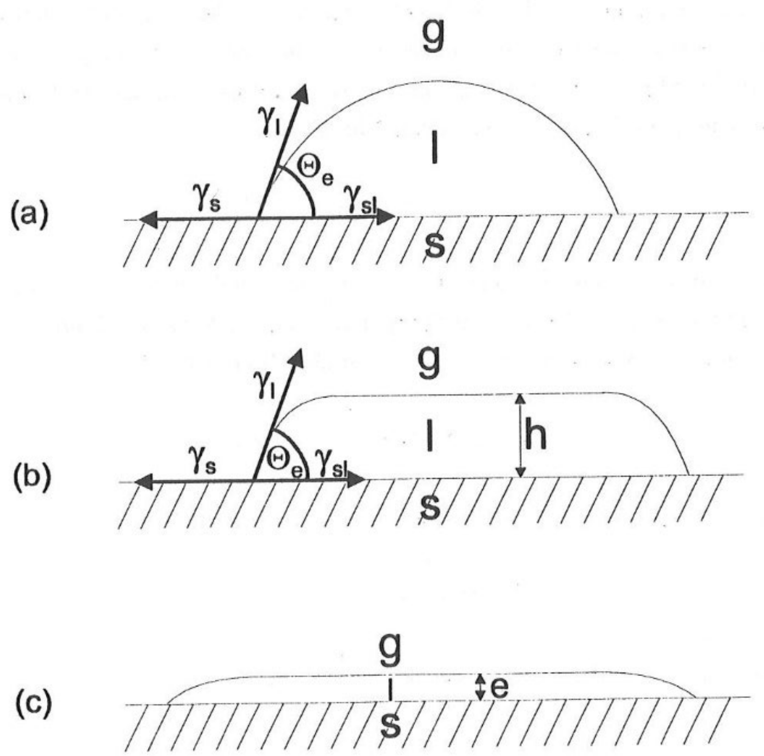

For small droplets the gravity can be neglected

R << k^{-1}

Droplets with increased volume are flatten by gravity resulting in a disc of height h

R >> k^{-1}

Complete wetting $S \geq 0$, spreading occurs until a film of thickness e and surface A is formed.

$e \approx 10 - 100$ Å

free energy of spreading: $\Delta F = -SA + P(h)A$

with S: spreading coefficient

P(h): long range Van der Waals forces

Thickness of Polymer Films

A random coil of a polymer chain with N monomers is placed on a smooth, hard, solid surface

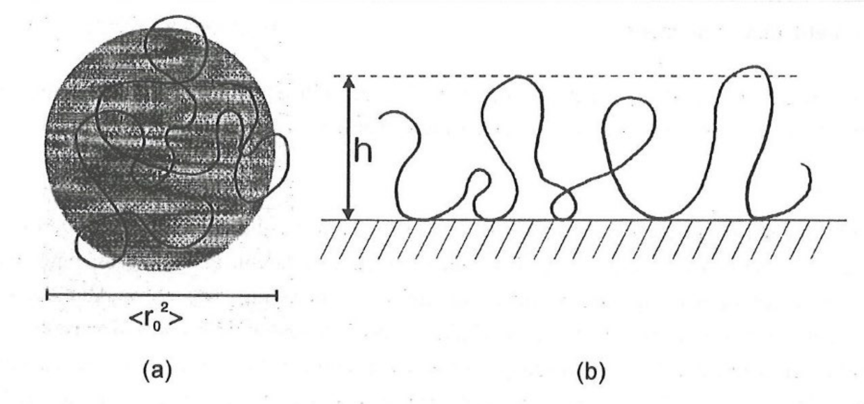

rms end-to-end distance is greater than the minimum film thickness e

film thickness is determined by the free surface energy F_s and additionally by the deformation energy F_{def}

$$\Delta F = \Delta F_s + \Delta F_{def}$$

$$\Delta F_{def} \cong \quad \alpha^{-2} + \ln\alpha^2 \qquad \text{with } \alpha = \sqrt{\frac{h}{N}}$$

Critical Surface Tension – Zisman plot

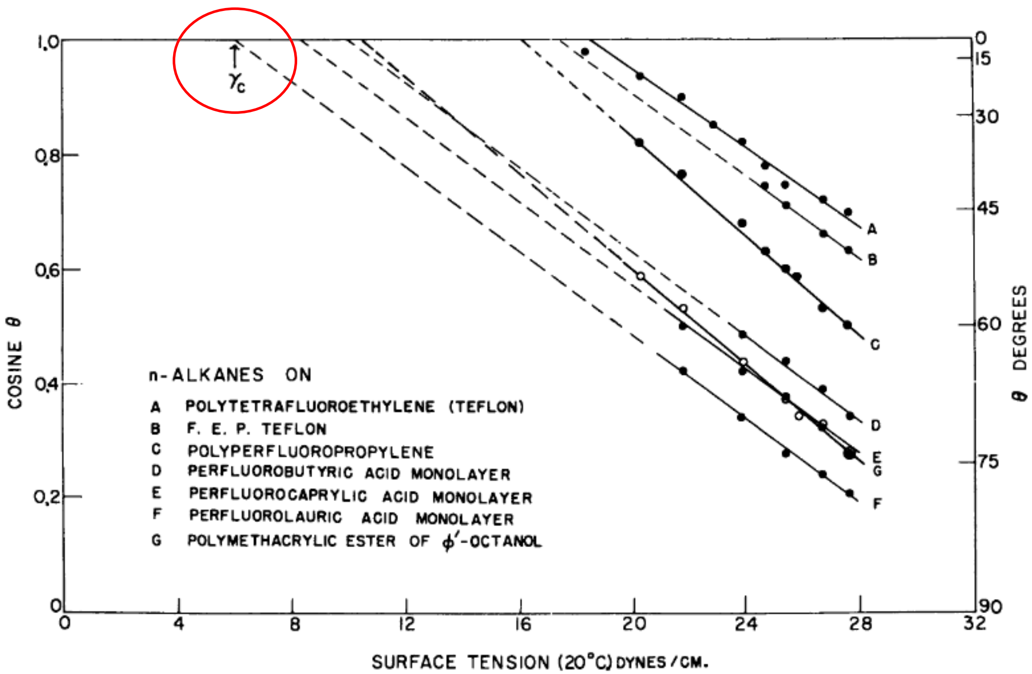

Semi-empirical linear relation between contact angles of a series of homologous liquids on a surface to the surface tension of these liquids.
The critical surface tension γ_c is obtained by extrapolation to complete wetting (cosθ = 1).

$$cos\theta = 1 + m(\gamma_l - \gamma_c)$$

TABLE 17.1. Values of Critical Surface Tension of Wetting (σ_c, mN cm^{-1}) for Various Materials

Solid	σ_c	Solid	σ_c
Teflon	18	Copper	60
Polytrifluoroethylene	22	Silver	74
Polyvinylidene fluoride	25	Silica (dehydrated)	78
Polyvinyl fluoride	28	Anatase (TiO_2)	92
Polyethylene	31	Graphite	96
Polystyrene	33	Lead	99
Polyvinyl alcohol	37	Tin	101
Polyvinyl chloride	39	Iron	106
Polyvinylidene chloride	40	Iron oxide(Fe_2O_3)	107
Polyethyleneterephthalate	43	Silica (hydrated)	123
Nylon 6,6	46	Rutile (TiO_2)	143

Influence of Surface Roughness

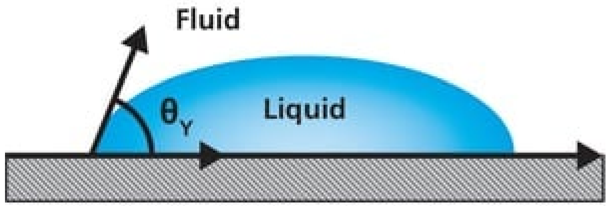

On the ideal surface, Young's equation applies, and the measured contact angle is equal to the Young's contact angle θ_Y

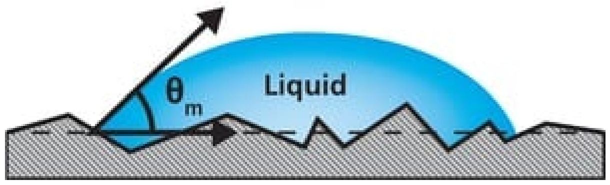

a real surface, the actual contact angle is the angle between the tangent to the liquid-fluid interface and the actual, local surface of the solid: θ_m

→ Models of Wenzel and Cassie/Baxter: a drop on a structured surface

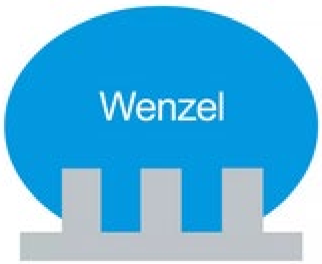

Influence of Roughness on Wettability

Θ > 90°: Surface roughness increases the hydrophobic character of a non-wetting surface

Θ < 90°: Surface roughness improves the wettabilitiy of a hydrophilic surface

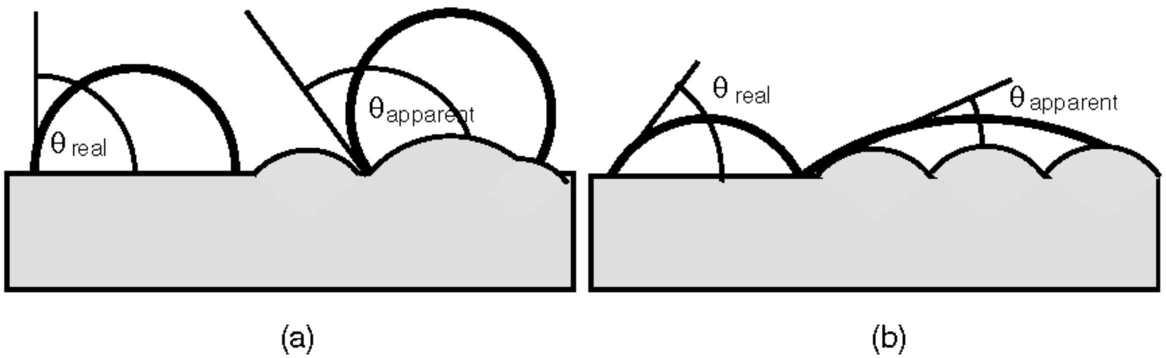

FIGURE 6.15. On a rough surface, the apparent contact angle can differ significantly from the "real" angle that would be observed on a molecularly smooth surface of the same material: (*a*) if the real contact angle is greater than 90°, the apparent angle will be even larger; (*b*) if the real angle is less than 90°, the apparent angle will be smaller.

Wenzel Model (1936)

$$\cos\theta^* = r\left(\frac{\gamma_{S2} - \gamma_{S1}}{\gamma_{12}}\right) = r\cos\theta_Y$$

with: r = $\dfrac{\text{real surface area}}{\text{projected flat surface area}}$

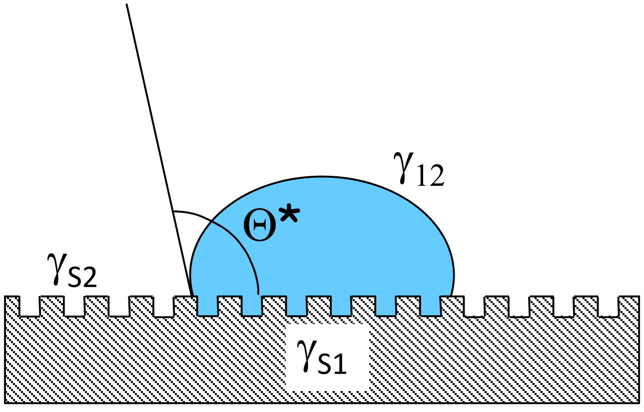

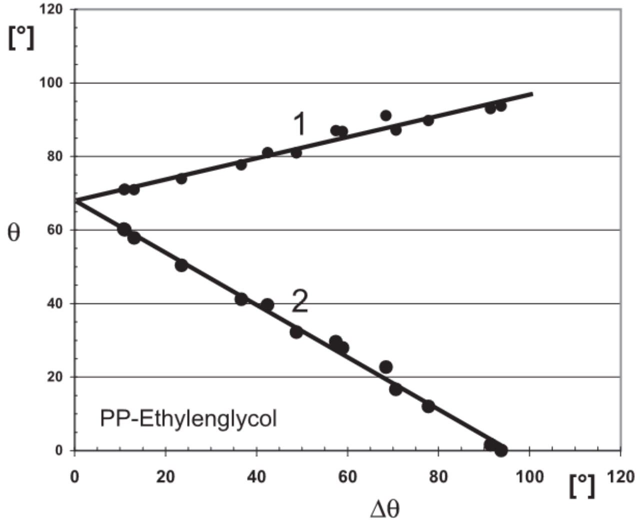

FIGURE 1 Advancing (1) and receding (2) contact angles measured with ethylene glycol on polypropylene samples with varying contact angle hysteresis due to varied roughness

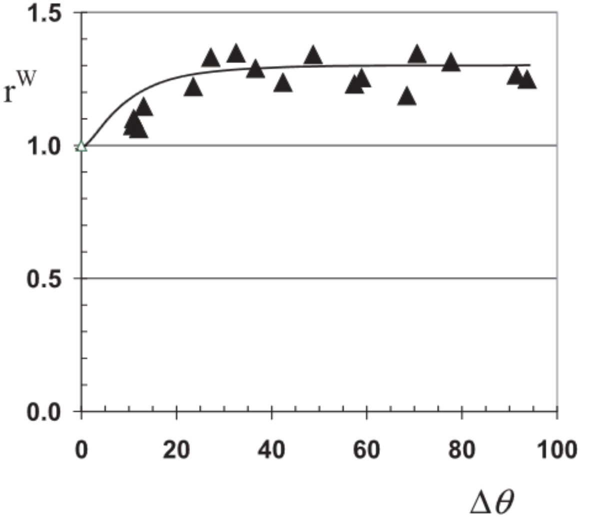

FIGURE 4 Roughness factor r^W, calculated by (11) from contact angle data, as a function of contact angle hysteresis $\Delta\theta$ for ethylene glycol on polypropylene for a series of samples varying roughness

R.N. Wenzel, *Ind. Eng. Chem.* **1936**, *28*, 988

H. Kamusewitz, W. Possart, Appl. Phys. A 76, 899–902 (2003)

Superhydrophobicity: Cassie – Baxter Model (1948)

This equation assumes a droplet on a porous surface where the pores are filled with air

$$\begin{aligned}\cos \Theta^* &= f \cos \Theta + (1 - f) \cos 180^\circ \\ &= f \cos \Theta - 1 + f \\ &= f (\cos \Theta + 1) - 1\end{aligned}$$

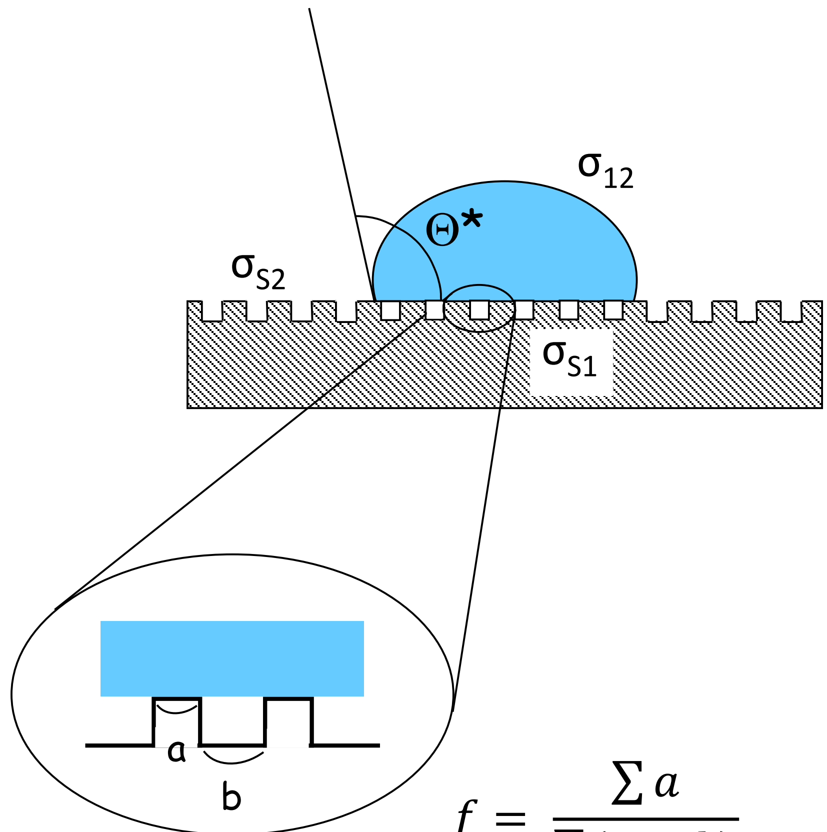

$$f = \frac{\sum a}{\sum (a + b)}$$

Where:
a = total area of solid – liquid interface
b = total area of liquid – air interface

A.B.D. Cassie, S. Baxter, *Trans. Farad. Soc.* **1944**, *40*, 546

Example Lotus Effect: Surface Structure and Wettability

Hierarchical surface structure

- Epidermal Cells
- Hydrophobic waxs crystals

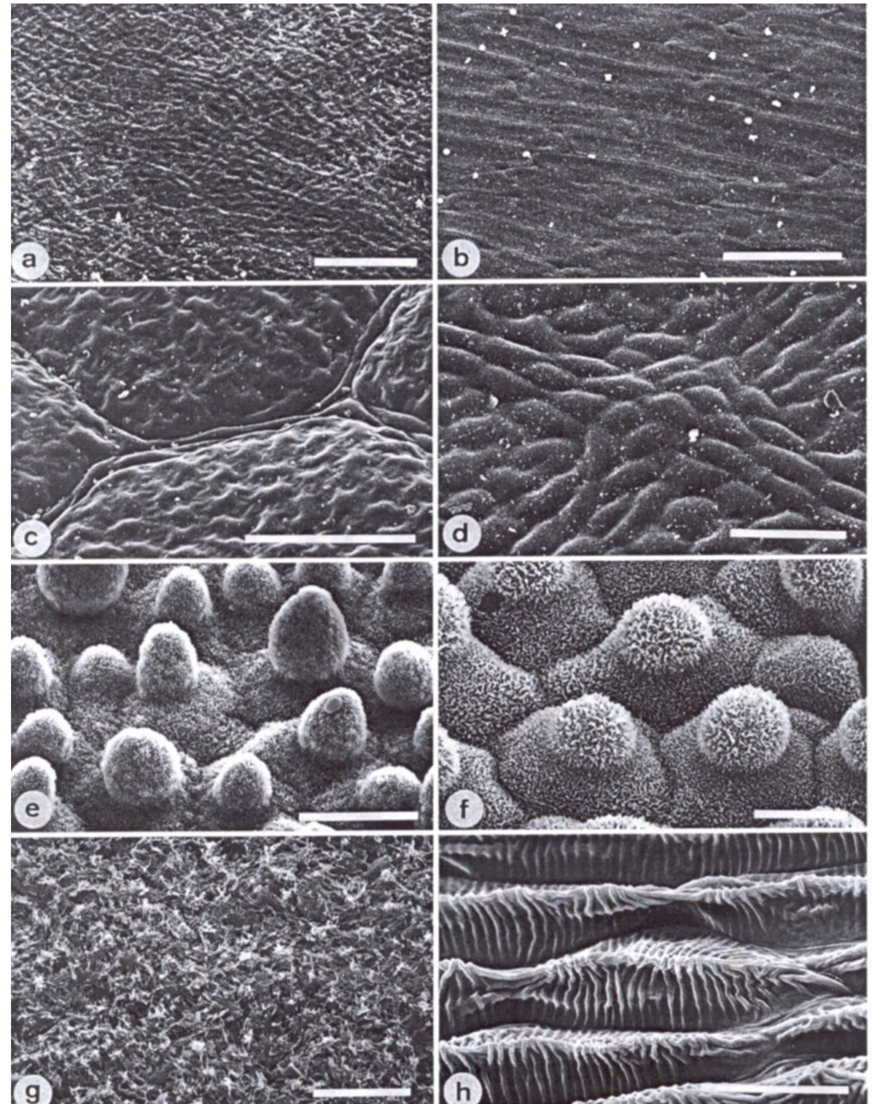

Table 1. Mean values (± SD) of 20 measurements of the static CA (°) on the adaxial leaf surfaces of the species used for contamination experiments

	Plant species	CA
b)	*Heliconia densiflora*	28.4 ± 4.3
a)	*Gnetum gnemon*	55.4 ± 2.7
d)	*Magnolia denudata*	88.9 ± 6.9
c)	*Fagus sylvatica*	71.7 ± 8.8
e)	*Nelumbo nucifera*	160.4 ± 0.7
f)	*Colocasia esculenta*	159.7 ± 1.4
g)	*Brassica oleracea*	160.3 ± 0.8
h)	*Mutisia decurrens*	128.4 ± 3.6

Fig. 1a–h. Scanning electron micrographs of the adaxial leaf surface of smooth, wettable (**a–d**) and rough, water-repellent (**e–h**) leaf surfaces. The smooth leaves of *Gnetum gnemon* (**a**) and *Heliconia densiflora* (**b**) are almost completely lacking microstructures while those of *Fagus sylvatica* (**c**) and *Magnolia denudata* (**d**) are characterized by sunken and raised nervature, respectively. The rough surfaces of *Nelumbo nucifera* (**e**) and *Colocasia esculenta* (**f**) are characterized by papillose epidermal cells and an additional layer of epicuticular waxes. *Brassica oleracea* leaves (**g**) are densely covered by wax crystalloids without being papillose, and the petal surfaces of *Mutisia decurrens* (**h**) are characterized by cuticular folds. *Bars* = 100 μm (**a–d**) and 20 μm (**e–h**)

W. Barthlott, C. Neinhuis, Planta **1997**, 202, 1

The Wenzel Model versus the Cassie Model

Wenzel:

$\cos \Theta^* = r \cos \Theta$

Cassie:

$\cos \Theta^* = f \cos \Theta - 1 + f$

$\cos \Theta_C = (f - 1)/(r - f)$
threshold value between the tow regimes

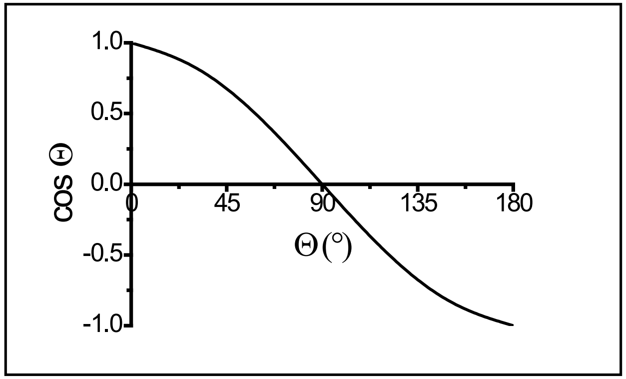

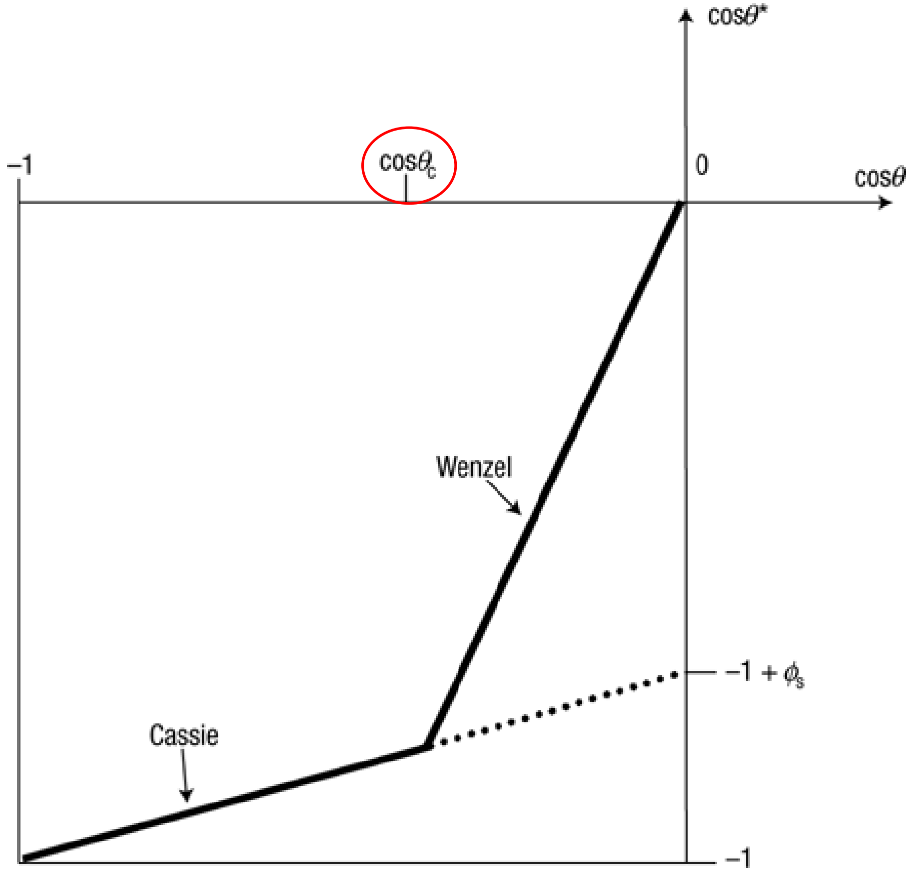

- Wenzel Regime: Moderately hydrophobic and rough surfaces
- Cassie Regime: Very hydrophobic and very rough surfaces (large Θ or r)

Figure from: A. Lafuma, D. Quéré, *Nature Mat.* **2003**, *2*, 457

The Wenzel Model versus the Cassie Model

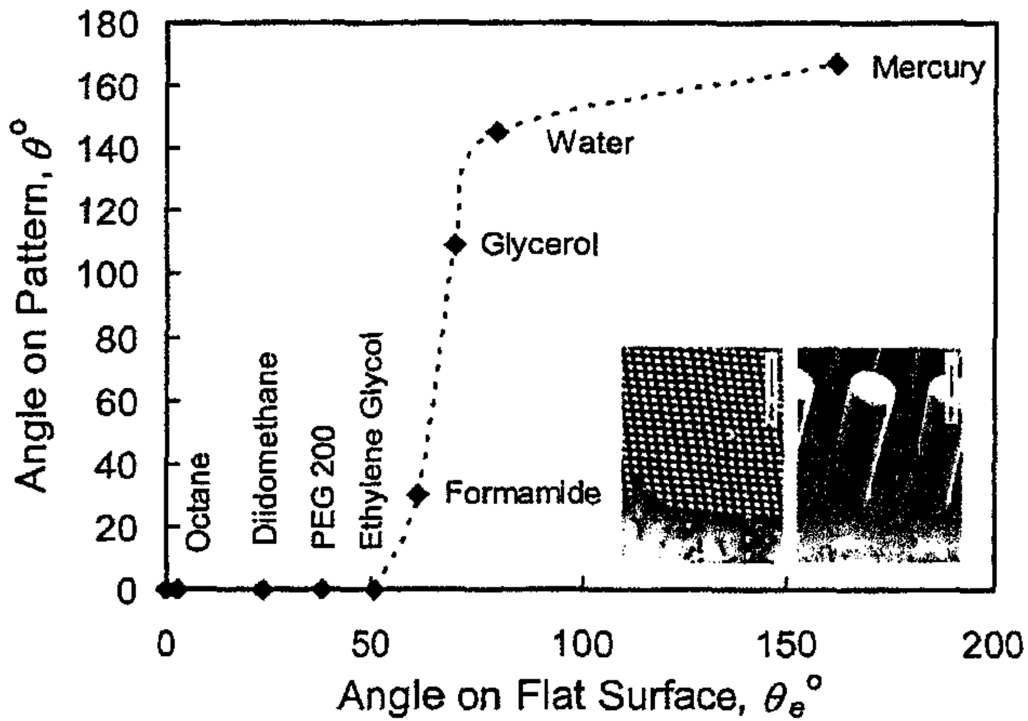

Fig. 2 Contact angles for a range of liquids on a textured SU-8 surface. The inset shows scanning electron microscope images of the lithographically structured surfaces showing a square lattice of 15 μm diameter cylindrical pillars with a 30 μm lattice parameter (view of a field of pillars and a close-up view of the pillars).

G. McHale, N.J. Shirtcliffe, M.I. Newton, *Analyst* **2004**, *129*, 284

The Wenzel Model versus the Cassie Model

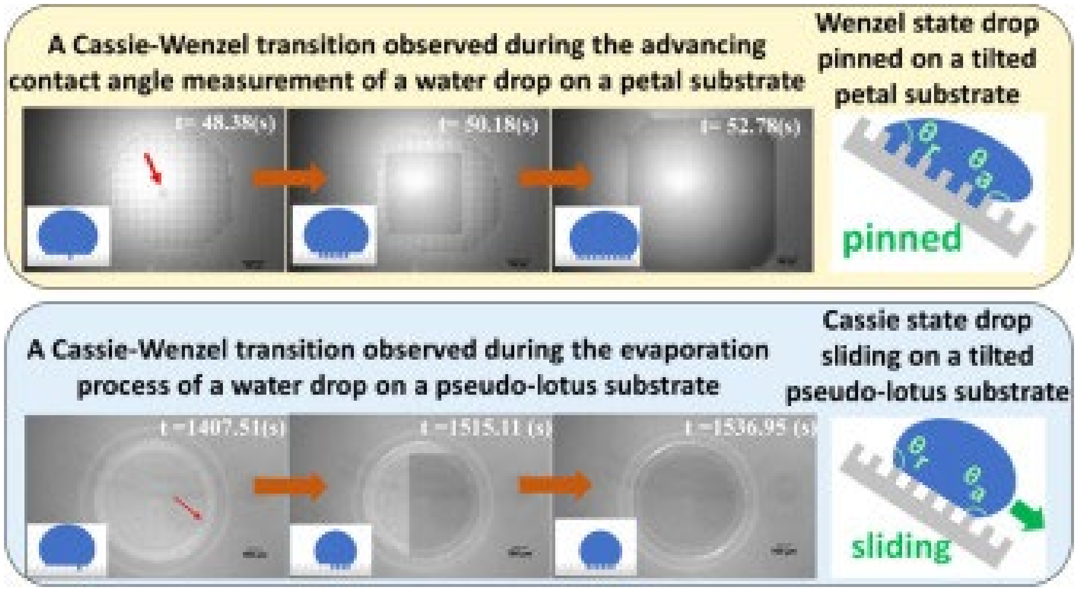

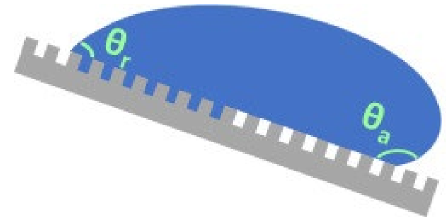

Schematic illustration of a water droplet in petal state on a single micro-scale roughness surface with a possible scenario that the front of the droplet, possessing ACA (θ_a), in Cassie state while the rear of the droplet, possessing RCA (θ_r), in Wenzel state.

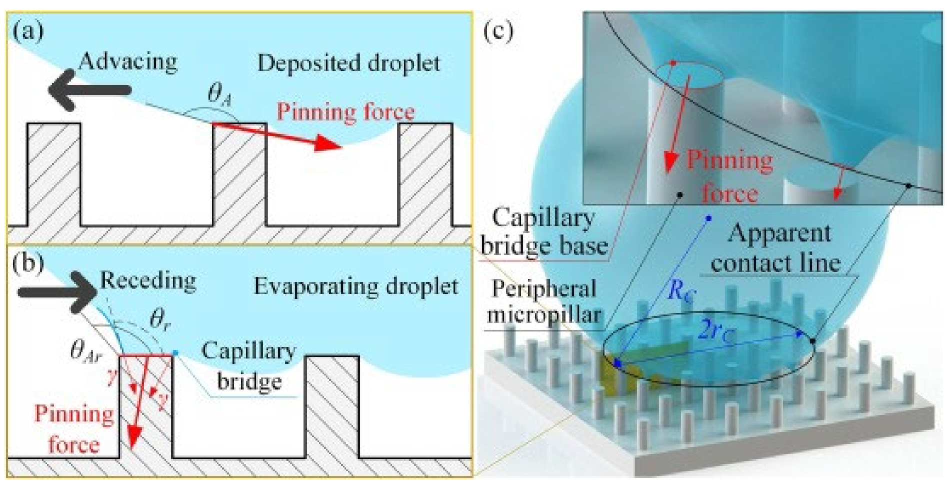

Hui-Ping Lin, Li-Jen Chen, Journal of Colloid and Interface Science 603 (2021) 539–549